International Journal of
Emerging Research in Management &Technology
ISSN: 2278-9359 (Volume-3, Issue-11)

Research Article | **November 2014**

Comparative Study in Optoelectronic Properties between Nano Gold/Porous Silicon Heterojunction Based on P and N-Type Crystalline Silicon

Hasan A. Hadi, Faten Sh. Zain Al-Abedeen
Department of Physics, College of Education,
Al-Mustanseriyah University,
Baghdad, Iraq

Abstract:

In this paper, investigations of structure and morphology properties of n and p-type porous silicon layer prepared by Photo-electrochemical etching (PECE) and electrochemical etching (ECE) were demonstrated respectively. The atomic force microscopy (AFM), x-ray diffraction (XRD) and optical microscopy investigations showed the influence of the substrate type on the structure, surface roughness and morphology porous silicon layer formation. The density current-voltage (J-V) measurements of Au/PS/n-Si and Au/PS/p-Si heterojunctions showed that they act as double-Schottky-diode behavior. In this work, both the responsivity and quantum efficiency of the porous silicon/c-Si heterojunctions were studied. The quantum efficiency of Au/PS/p-Si HJ was more than 100% comparing with that of Au/PS/n-Si HJ, which to be more than 80% at near ultra violet –visible region. Moreover, effects of the wafer Si substrate type on the responsivity and quantum efficiency of Au/PS/c-Si HJs were discussed and analyzed.

Keywords: Porous silicon; XRD; AFM; PECE; ECE; Responsivity; Quantum efficiency

I. INTRODUCTION

Among porous semiconductors, porous silicon (PS) has been investigated intensively; however the instability of physical properties has prevented it from large scale application [1]. Porous silicon is a very promising material due to its excellent properties and compatibility with silicon based microelectronics with reduced fabrication cost [2]. It is important to deposit metals and change chemical composition of the PS surface with metal atoms to form a good electrical contact for microelectronics and photo electronics [3]. The nano silicon is intensely photoluminescent in the visible range at room temperature (RT) and it is extremely sensitive to the ambient composition, leading to possible optoelectronic, biomedical and sensor applications [4]. Success of PS in application areas depended on how challenges in seeking suitable metallization could be overcome [5]. It is known that the surface properties of the transparent conducting films influence their optical and electrical properties which are important factors for applications in optoelectronic devices in principle [6]. There are many research elsewhere, has been studied electrical, electronic and structural properties of Au on bulk silicon (c-Si) and with different interfacial layers such as not limited [7-10], but in this work the porous silicon layer (PS) between the gold metal and bulk silicon (c-Si) in both types was used as interfacial layer. In this work, the synthesis and characterization of electrochemically anodized porous silicon layers is done. The photocurrent density-voltage characteristics of Au Schottky contact on p and n-Si with different power densities was reported. Also, the figures of merit of gold/nano-crystalline porous silicon/n and p-crystal silicon photodiode such as spectral responsivity and quantum efficiency were investigated and analyzed.

II. EXPERIMENTAL DETAILS

In figure (1-a) a Photo-electrochemical etching (PECE) was carried out in illuminating the front-side substrate surface using the red diode laser of 650nm and power of 30mW to produce porous silicon PS on like mirror surface n-type. Electrochemical etching (ECE) (see figure (1-b)) was performed in dark to produce PS on like mirror surface p-type. Porous silicon layer formation on monocrystaline Si substrate with a resistivity of (10-15) and (11-14) Ω-cm corresponding to a doping density $(1.34 \times 10^{15} - 8.91 \times 10^{14})$ and $(4.03 \times 10^{15} - 3.15 \times 10^{14})$ cm^{-3} for p-type and n-type respectively.

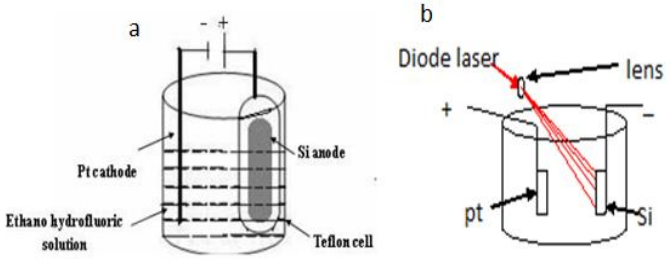

Figure (1): (a) Schematic diagram of electrochemical anodization system (ECE), (b) Schematic diagrams of photo-electrochemical etching (PECE) [5].

The (111) crystallographic orientation silicon wafers n and p type, were used. Silicon wafers with Al thin layer deposited onto a back-side were located in an electrochemical cell. The anodization in a simplest electrochemical plastic cell and was generated by Pt assisted electrodes chemical etching with 40% HF and methanol (98%) solution 1:1 (v: v) at etching current densities of 30 mA/cm^{2}and anodization time of 30 min. A scheme of heterostructures Au/PS/c-Si devices for n and p type wafer silicon is shown in figure (2).

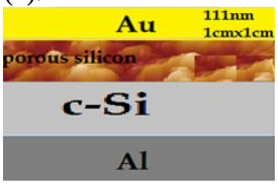

Figure (1): Diagram of the cross section of Au/PS/Si/Al heterostructures Schottky contact.

After PECE and ECE process, samples were cleaned with methanol and distilled water. The top one semitransparent window thermally evaporated and Schottky diode contact was made by evaporation of gold on the top of PS layer at the same condition. The samples are prepared in sandwich configuration, top Au/PS/c-Si/bottom Al, the top one semitransparent electrode thermally evaporated with 111nm and the bottom electrode is coated with 0.8μm Aluminum layer before the anodization process. Here Ohmic contacts on both PS and bulk silicon were made by deposition of high purity Al films by using thermal resistive technique under vacuum pressure of 10^{-6} torr, using an evaporation plant model "E306 A manufactured by Edwards high vacuum". After evaporation process, thickness of evaporated film on a glass substrate was measured using gravimetric method. In gravimetric method, "Mettler AE-160 digital with accuracy of 10^{-4} gm" is used to weight the samples. The surface profiles were analyzed by atomic force microscopy (AA 3000 Scanning Probe Microscope AFM system). The I-V tracing for the PS / Au junction was conducted with the help of an using UNI-T UT61E Digital Multimeters and dc. power supply type LONG WEI DC PS-305D 30 ranges (0-10) V. Measurements of photocurrent of heterojunction were done under white light of different illumination power densities supplied by a halogen lamp with power of 150 W, which was connected to a Variac and calibrated by power meter. The photosensitivity of the photo-detector is investigated in the wavelength with the aid of Joban-Yvon monochromatic and standard Si power meter.

III. RESULTS AND DISCUSSION

XRD spectra of two bulk (c-Si) substrates and porous silicon layer formed on n-Si and p-Si samples have been presented in figure (3-a,b,c and d). Comparing between figure (3-a) and (3-c), showed that the effect of substrates type creates high difference in XRD spectrum (peak intensity and broadening). In table (1) the full width at half maximum (FWHM) of p-type XRD pattern was large than of n-type, is suggestive of smaller crystallite size of p-type. The green size of n-Si was to be 215nm and 155nm for p-type. When crystal size is reduced toward nanometric scale, then a broadening of diffraction peaks is observed and the width of the peak is directly correlated to the size of the nanocrystalline domains [11]. The size of crystal silicon was estimated from XRD spectra using Sherrer's formula [12].

$$L=k\lambda / \Delta(2\theta)\ COS\theta \qquad (1)$$

Where λ is the wavelength of the X-rays, θ is the Bragg diffraction angle at the peak position in degrees, Δ(2θ) is the FWHM in radian, and k is a correction factor. The value of k is usually chosen to be 0.9 for Si films.

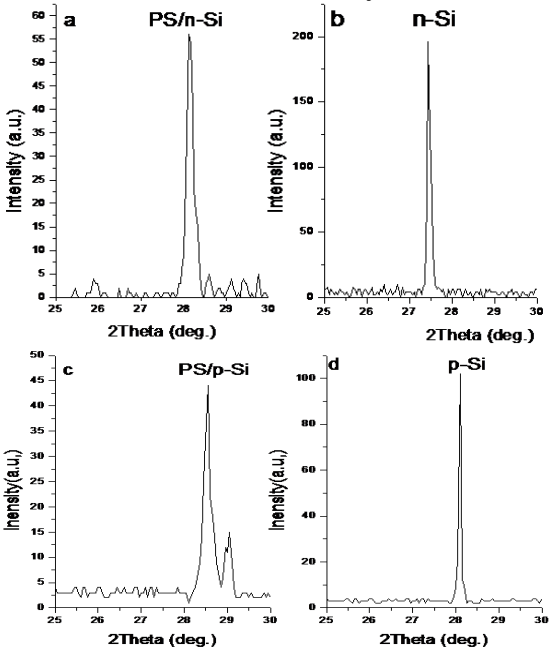

Figure (3): (a) XRD spectra of PS sample anodized on (b) n-type silicon and (c) XRD spectra of PS sample anodized on (d) p-type silicon at constant current density of 30mA/cm^2.

Table (1): crystalline size of porous silicon

Porous layer type	FWHM(c-Si)	FWHM (PS)	L(nm)
PS/n-Si	0.1012	0.1198	215
PS/p-Si	0.1086	0.1453	155

In figure (4-a and b) pictures of the surface of PS formed at different type of substrate are shown, using (111) wafer and at the same preparing condition. Optical microscopy images showed different color resulting from broadening of the band gap energy (quantum confinement). It occur when there is a decrease in the crystallite size for p and n type Si and that agreement with our results of crystallite size from XRD measurement. The left inset of figure (4-a and b) show the images of porous layer formed on n-Si and p-Si, and it is possible to confirm the effect of substrate type on the behavior of morphology of the PS.

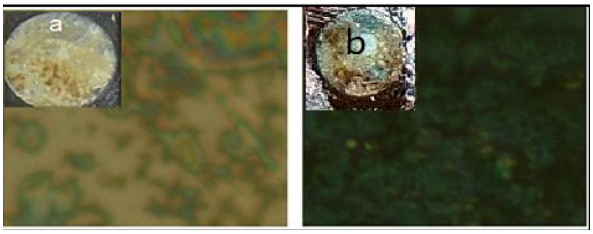

Figure (4): (a) PS/n-Si surface image by optical microscopy , (b) PS/p-Si surface image by optical microscopy and left inset Figure(a and b) show the porous silicon layer image by camera digital HD Samsung 5x on n and p –Si substrate respectively.

Compare to figure (4-a) and (4-b), we can see that the porosity of wafer is not uniform in (a) sample because H_2bubbles created on the surface preventing further silicon dissolution in n-Si wafer. The electrochemical etching in n-Si wafer is required more holes as compared to the p-Si wafer, so the semiconductor must be illuminated. The morphology and structure of porous silicon layer were investigated as shown in figures (5) and (6) for p and n-type wafer silicon respectively. A 3D and 2D topographic image of porous silicon appears as peaks with pyramid-shaped bases spread over a wide area surface. The surface of the PS layer consists of inhomogeneous and large number of irregularly shaped 'pores and voids' distributed randomly over the entire surface. Root-mean-square (RMS) surface roughness is a commonly accepted parameter to describe surface. It is typically used to quantify variations in surface elevation, the RMS (root mean square) roughness for PS was found to be 11.4nm and 22.4nm for p and n-type respectively. The Sz. (Ten Point height) of p and n-type were found to be 76.9 nm and 133nm respectively. Depending on the wafer type, geometry of the pores changed and different green size can be obtained. Our results show the nanometric scale made from p-type substrate .while the range of thickness to micrometric scale obtained from illuminated n-type substrate and that agree with [13]. These different morphologies are the result of different pore formation mechanisms. Many mechanisms are thought to contribute to the electrochemical pore growth process in silicon, and the morphology resulting from a given experiment is usually determined by a combination of several of these [14]. This roughness is expected to be caused by inhomogeneous of the substrate and electrolyte composition, and seems to increase with layer thickness. So may be these roughness leads to reduce of light reflection and possibility of its application such as photo-detector.

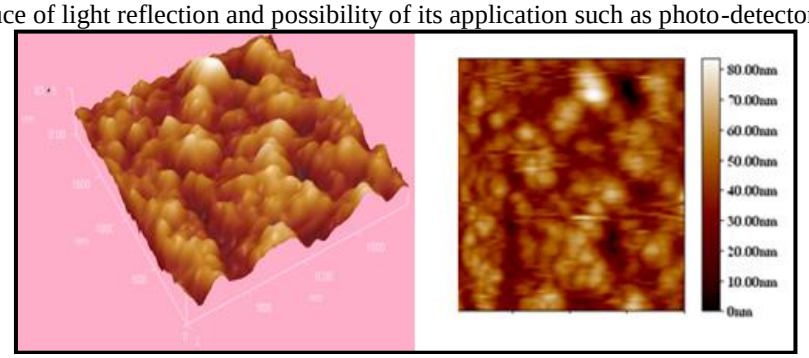

Figure (5): 3D and 2D Surface AFM image of the PS layer on p-Si substrate (2µm×2µm).

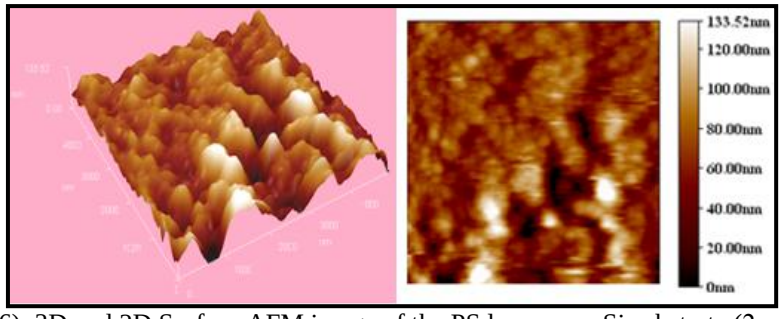

Figure (6): 3D and 2D Surface AFM image of the PS layer on n-Si substrate (2µm×2µm).

Figures (7) and (8) show forward and reverse density current–voltage characteristics of Au/PS/n-Si and Au/PS/p-Si heterojunctions measured under dark and illumination with different light power densities. The photocurrent is measured for light power densities of 0.9–9 W/cm^2. The equation, which describes the current as a function of the applied voltage of the junction can be expressed as [15]:

$$I = I_{\circ}[\exp\left(\frac{qV}{nKT}\right) - 1] \qquad (2)$$

The current flowing depends on two parts: the one which is flowing from the metal to the semiconductor minus the one which is flowing from the semiconductor to the metal. The current starting at a low voltage corresponds to that of a typical thermionic emission. In linear region, thermionic emission and carrier velocity increases. When light power density is increased, the photocurrent is increases due to generation of electron–hole pairs. No soft breakdown has been noticed in the prepared heterojunction at voltage lees than $\mp$5V in double Schottky device. The maximum photocurrent density at the bias of -9V were (644.2, 1178.2, 1830.2and 2094.2) μA/cm^2 and (480, 1236, 3664and 4444) μA/cm^2 for n and p –type illumination by (0.9, 2, 5 and 9) mW/cm^2 power densities respectively. The results showed reduced resistance with increasing photon energy of the illuminating light for both type samples, likely due to increased generation of electron hole-pairs. It can be seen from figures (7) and (8) that the current value at a given voltage for PS/p-Si HJ under illumination is higher than that the PS/n-Si HJ. This indicates that the light generates carrier-contributing photocurrent due to the production of electron–hole pairs as a result of the light absorption in p-type was better than from n-type Si substrate. The saturation current density, measured from semi log I-V plot, were 0.09 μA and 0.01 μA for n and p-type respectively .The ideality factor was calculated from equation (1) which found to be 3.3 and 7.2 for p and n- type respectively. This can be described to the surface states , trapping centers in homogeneities of film thickness, interface states, series resistance, tunneling process and non-uniformity distribution of the interfacial charges in n-type large than in p-type .

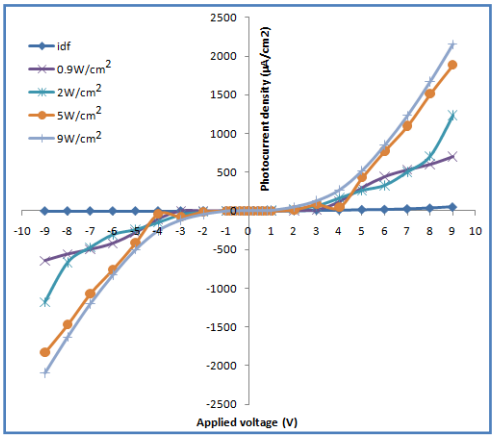

Figure 7: Dark and Photo-current of PS/n-Si heterojunction as function of forward and reverse bias illuminated for different power density.

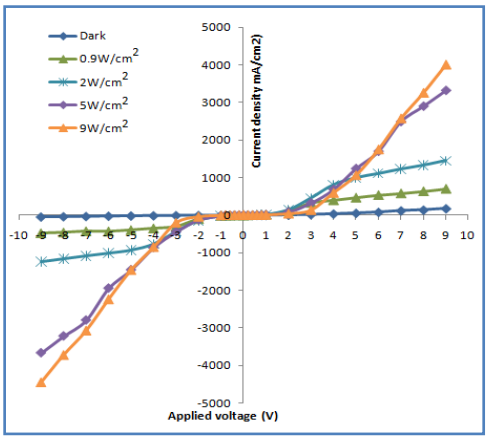

Figure (8): Dark and Photo-current of PS/p-Si heterojunction as function of forward and reverse bias illuminated for different power density.

Because of symmetric behavior of photocurrent in forward and reverse, figure (5) showed double soft avalanche regions at $\pm$5V bias. These results refer to the silicon/porous, silicon heterojunction act as double-Schottky-diode and the photocurrent generation depends on the wavelength of the illumination light. Figure (9-a and c) represent the ratio of the photocurrent to the incident light power at a given wavelength of the photo-detector fabricated. It is noted that the responsivity curve (Figure (9-a)) shows two distinct peak, the first one (corresponding to the near infrared-visible spectral region) shows an increase in responsivity with decrease wavelength, attains the maximum value (0.44W/A) at 700 nm (the absorption edge toward n-Si/Al side of Au/PS/n-Si/Al heterojunction). The lower responsivity (0.28W/A) at

the shorter wavelength region (near UV at 450 nm) due to the absorption of the light in porous layer (toward PS/n-Si side of Au/PS/n-Si/Al heterojunction) near the interface, which has large amount of surface recombination of the photo-generated carriers. the absorption of short wavelength occurs within the PS layer and the large wavelength is absorbed at the interface of Si and PS [16]. The maximum of responsivity Au/PS/p-Si heterojunction happened at near UV-Visible region (450nm), that means the most of absorption take place in Au/PS interface toward porous layer as shown in figure (9-c). These measurements were obtained using a monochromatic as the light source and the result of bulk silicon/Al contact has a lower sensitivity compare with Au/porous silicon contact. This is due to the band gap of silicon is smaller than that of gold/porous silicon (eV). Therefore, the side of porous silicon has a higher sensitivity .The value of quantum efficiency was estimated using the following equation [17]:

$$Q.E = 1240 \frac{R_\lambda}{\lambda_{nm}} \qquad (3)$$

Where R_λ is the responsivity of a photodiode which is given as the measured current per incident power, λ is the wavelength of light. The maximum values of quantum efficiency in two peaks were 81% and 77% at 700nm and 450nm respectively. The high value due to scattering and transmission at the roughness of porous and porous bulk interfaces leads to reduce of light reflection. This parameter has its significant role in order to enhance the light. The quantum efficiency of Au/PS/p-Si HJ was more than 100% at same region (near UV-Visible), this was compared with that of Au/PS/n-Si HJ which was more than 80% and the low quantum efficiency regions may be result to the large numbers of surface traps in PS/n-Si interface surface as a result of the geometrical non-uniformity of PS/n-Si interface should be higher in the PS/p-Si interface as well. Also Balagurov *et al.* reported that the high value of quantum efficiency (large then 100%) come from the avalanche effect inside the porous silicon and later is generated by the voltage drop in porous silicon which is intrinsic and as narrow as silicon wire [18].

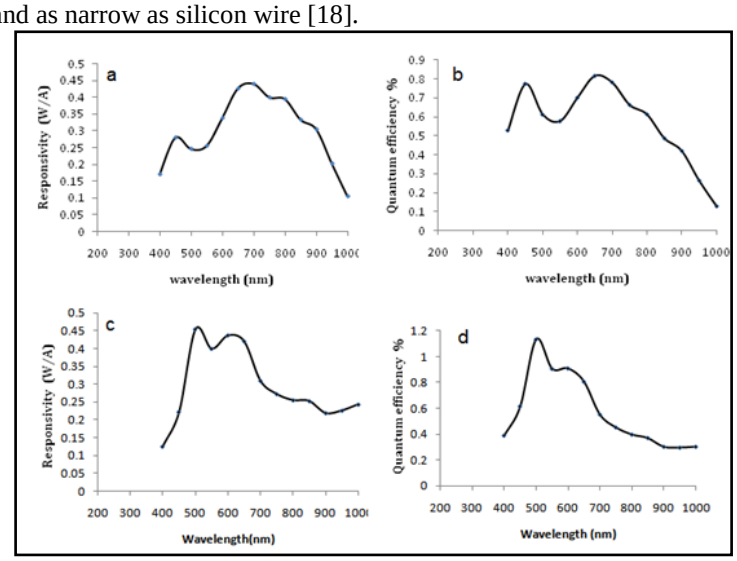

Figure (9): Responsivity and Quantum efficiency as a function of various incident wavelengths for Au/PS/n-Si/Al (a and b) and (c and d) for Au/PS/p-Si/Al structure

IV. CONCLUSIONS

Morphological studies of porous silicon formed on n and p type silicon have been performed. The AFM have been used to characterize porous based surface. Porous silicon substrates, etched with different type of wafers silicon, which is p and n-Si were characterized by XRD, optical microscopy and atomic force microscopy (AFM).

XRD spectra showed broadening of diffraction peaks and the width of the peak is directly correlated to the size of the nanocrystalline domains. Optical microscopy images showed different color resulting from broadening of the band gap energy which is occurs as a result of the decreasing in the crystallite size for p and n type Si.

The results showed reduced resistance with increasing photon energy of the illuminating light for both type samples, likely due to increased generation of electron hole-pairs. The saturation current density were 0.09 μA and 0.01 μA for n and p-type respectively

In this work Au/PS/n-Si and Au/PS/p-Si heterojunction photo diode was demonstrated with high quantum efficiency in the Near UV and visible regions.

REFERENCES

[1] F.K.Yam and Z.Hassan, "The investigation of dark current reduction in MSM photodetector based on porous GaN", journal of optoelectronics and advanced materials, **10**(3) 545 – 548 (2008).

[2] R.S. Dubey. "Electrochemical Fabrication of Porous Silicon Structures for Solar Cells", Nanoscience and Nanoengineering , **1**(1) 36-40 (2013).

[3] V. Iancu, M. L. Ciurea, I. Stavarache, V. S. Teodorescu, "Phototransport and photoluminescence in nanocrystalline porous silicon", journal of optoelectronics and advanced materials, **9**(8) 2638 – 2643 (2007).

[4] Kadir Esmer, Ersin Kayahan , "Influence of alkali metallization (Li, Na and K) on photoluminescence properties of porous silicon", Applied Surface Science **256**, 1548–1552 (2009).

[5] H. A. Hadi, R. A. Ismail and N. F. Habubi, "Optoelectronic properties of porous silicon heterojunction photodetector", Indian J. Phys., **88**, 59–63(2014).
[6] T.Van ,L.Dinh, "Changes in the electronic properties of silicon nanocrystals as a function of particle size". Phys Rev Lett **80**(17), 27 (1998).
[7] Zuo, Guanglei Cui, Yi Shi, Yousong Liu and Guangbin Ji, "Gold-thickness-dependent Schottky barrier height for charge transfer in metal-assisted chemical etching of silicon", Nanoscale Research Letters, **8**:193 (2013).
[8] E. Bhattacharya, P. Ramesh and C. Suresh kumar, "Studies on Gold/Porous Silicon/Crystalline Silicon Junctions", Journal of Porous Materials **7**, 299–301 (2000).
[9] T. Tunç I.dökme Ş. Altindal and I.uslu, "Temperature dependent current-voltage (I-V) characteristics of Au/n-Si (111) Schottky barrier diodes (SBDs) with polyvinyl alcohol (Co, Ni-Doped) interfacial layer" Optoelectroncs and advanced materials rap dcommucaons, **4**(7), 947-950 (2010).
[10] S. Alialy, H. Tecimer, H. Uslu and Ş. Altındal, "A Comparative study on electrical characteristics of Au/N-Si Schottky diodes, with and Without Bi-Doped PVA interfacial layer in dark and under illumination at room temperature," J Nanomed Nanotechol, **4**:3 (2013).
[11] Lorusso, A. V. Nassisi, G. Congedo, N. Lovergine, L. Velardi, P. Prete, "Pulsed plasma ion source to create Si nanocrystals in SiO2 substrates", Applied Surface Science, **255**, 5401-5404 (2009).
[12] A.A. Salman F. I. Sulta and U.M. Nayef "Structural, Chemical and Morphological of Porous SiliconProduced by Electrochemical Etching" Eng.&Tech.Journal, **30**(5) 856-868(2012).
[13] R. Jarimavičiūtė-Žvalionienė1, V. Grigaliūnas, S. Tamulevičius1,2, A. Guobienė1,2Fabrication of Porous Silicon Microstructures using Electrochemical Etching ISSN 1392–1320 Materials Science (Medžiagotyra). **9**(4) 317-320 (2003).
[14] Porous Silicon in Practice: Preparation, Characterization and Applications, First Edition. Michael J. Sailor. Wiley-VCH Verlag GmbH & Co. KGaA (2012).
[15] Z.Ahmad, M.H.Sayyad, M.Yaseen, and M. Ali,"Investigation of 5, 10, 15, 20-Tetrakis(3',5'-Di-Tert-Butylphenyl)Porphyrinatocopper(II)forElectronics Applications", World Academy of Science, Engineering and Technology **76** 811-814(2011).
[16] S. V. Svechnikov, E. B. Kaganovich, and E. G. Manoilov, "Photosensitive porous silicon based structures," Semiconductor Physics, Quantum Electronics & Optoelectronics, **1**, (1) 13-17. (1998).
[17] S.M.Sze and K.Kwok,"Physics of Semiconductor Devices," Third Edition Published by John Wiley & Sons, Inc., Hoboken, New Jersey, 614-618 (2007).
[18] Balagurov L. A. , Bayliss S.C., Yarkin D. G., Andrushin S. Ya., Kasatochkin V. S. , Orlov A. F. and Petrova E.A., "Low noise photosensitive device structures on porous silicon " Solid state Electron. 47, 2003, P.65.

